MASARYKOVA UNIVERZITA

Přírodovědecká fakulta

Ústav teoretické fyziky a astrofyziky

Interakce temné hmoty a stelárních hal ve slupkových galaxiích

Bakalářská práce

Zuzana Petrovská

Vedoucí bakalářské práce:
RNDr. Bruno Jungwiert, Ph.D.

Brno 2018

Bibliografický záznam

Autor:	Zuzana Petrovská Přírodovědecká fakulta, Masarykova univerzita Ústav teoretické fyziky a astrofyziky

Název práce:	Interakce temné hmoty a stelárních hal ve slupkových galaxiích
Studijní program:	Fyzika
Obor:	Astrofyzika
Vedoucí práce:	RNDr. Bruno Jungwiert, Ph.D.
Akademický rok:	2017/2018
Počet stran:	viii + 39
Klíčová slova:	slupkové galaxie, temná hmota, sub-halo, MOND, Lambda-CDM

Bibliographic record

Author:	Zuzana Petrovská Faculty of Science, Masaryk University Department of Theoretical Physics and Astrophysics

Title of Thesis:	Interactions of dark matter and stellar halos in shell galaxies
Degree Programme:	Physics
Field of study:	Astrophysics
Supervisor:	RNDr. Bruno Jungwiert, Ph.D.
Academic Year:	2017/2018
Number of Pages:	viii + 39
Keywords:	shell galaxies, dark matter, sub-halo, MOND, Lambda-CDM

Abstrakt

Téma problému chybějící hmoty se v posledních desetiletích stalo frekventovaným impulzem na odbornou diskuzi. Tento problém obecně vysvětlují dva modely. Prvním z nich je MOND, který vybízí k úpravě tradičních fyzikálních rovnic. Druhým z nich je model Lambda-CDM, který nevyžaduje úpravu původních rovnic, naopak přichází s myšlenkou existence neviditelné substance, temné hmoty. Jedním z mnoha způsobů, jak pozorovat interakci temné hmoty je na galaktických útvarech, které jsou slupky v slupkových galaxiích. Podle předpokladu, že model Lambda-CDM je správný, tuto slupkovu galaxii obklopuje halo tvořeno temnou hmotou. Toto halo může mít vlastní strukturu, tedy může být tvořeno shluky temné hmoty, tzv. sub-haly.

Simulace vykonané v této práci popisují vznik slupkové galaxie, pohyb takového sub-hala v potenciálu slupkové galaxie a přechod sub-hala minimálně jednou ze vzniklých slupek. Výsledky neprokázaly žádné změny v rozložení slupek po průchodu sub-halem. Tyto výsledky rozhodně nevyvrací existenci temné hmoty a podporují model Lambda-CDM.

Abstract

The missing mass problem topic has been a frequent subject of specialist debate for a few decades. Generally two models explain this problem. The first one is MOND which calls for editing traditional physical equations. The second model is Lambda-CDM which does not call for any changes in the original equations, but comes in with an idea of existence of an invisible substance called dark matter. One of many variants to observe interactions of dark matter is to observe these interactions on galactic shapes such as shells of shell galaxies. Assuming that the Lambda-CDM model is valid, there is a dark matter halo enveloping such a shell galaxy. This halo can have its own structure which means it can be made of sub-halo clumps.

Simulations created in this thesis describe a formation of a shell galaxy, motion of a sub-halo in the shell galaxy potential and a sub-halo transit across at least one of the created shells. The results do not demonstrate any changes in the shell galaxy distribution after the sub-halo transit. These results do not disprove the dark matter existence and strengthen the Lambda-CDM model.

MASARYKOVA UNIVERZITA
Přírodovědecká fakulta

ZADÁNÍ BAKALÁŘSKÉ PRÁCE

Akademický rok: 2017/2018

Ústav: Ústav teoretické fyziky a astrofyziky

Studentka: Zuzana Petrovská

Program: Fyzika

Obor: Astrofyzika

Ředitel *Ústavu teoretické fyziky a astrofyziky* PřF MU Vám ve smyslu Studijního a zkušebního řádu MU určuje bakalářskou práci s názvem:

Název práce: Interakce temné hmoty a stelárních hal ve slupkových galaxiích

Název práce anglicky: Interactions of dark matter and stellar halos in shell galaxies

Oficiální zadání:
Hvězdné slupky, obloukovité útvary ve hvězdných halech galaxií, jsou výsledkem destruktivních srážek, při nichž dvě galaxie splynou v jednu. Radiální rozložení a geometrie slupek v sobě obsahují informaci o gravitačním poli galaxie, v rámci standardního Lambda-CDM scénáře kosmologického scénáře tedy i informaci o rozložení temné hmoty v galaktických halech. Cílem práce je studium interakcí temné hmoty a hvězdných slupek prostřednictvím simulací.

Literatura:
BINNEY, James a Michael MERRIFIELD. *Galactic astronomy*. Princeton: Princeton University Press, 1998. 796 s. ISBN 0-691-02565-7.

BINNEY, James a Scott TREMAINE. *Galactic dynamics*. 2nd ed. Princeton: Princeton University Press, 2008. xvi, 885. ISBN 9780691130279.

Jazyk závěrečné práce: angličtina

Vedoucí práce: RNDr. Bruno Jungwiert, Ph.D.

Datum zadání práce: 20. 2. 2018

V Brně dne: 17. 4. 2018

Souhlasím se zadáním (podpis, datum): 23. 04. 2018

Zuzana Petrovská **studentka**	RNDr. Bruno Jungwiert, Ph.D. **vedoucí práce**	prof. Rikard von Unge, Ph.D. **ředitel Ústavu teoretické fyziky a astrofyziky**

Poďakovanie

Touto cestou by som sa chcela poďakovať vedúcemu mojej bakalárskej práce za skvelú tému na spracovanie, pánovi RNDr. Brunovi Jungwiertovi, Ph.D. a taktiež za pomoc pri spracovaní aj pri neľahkých chvíľach. Nesmierna vďaka patrí môjmu kolegovi Vaškovi Glosovi, ktorý mal so mnou obrovskú dávku trpezlivosti a pomohol mi vysvetliť záležitosti ohľadom práce, ktoré mi boli dovtedy skryté. Za pomoc v jeho voľnom čase mu nesmierne ďakujem. Obrovské poďakovanie patrí aj mojim spolužiačkam, Tonke Vojtekovej a Jarke Seckej, ktoré mi vždy dodávali obrovskú motiváciu, priestor na diskusiu a taktiež mi pomohli sa dostať najmä tu, k odovzdávaniu bakalárskej práce.

V neposlednom rade patrí nesmierna vďaka mojej rodine, ktorá mi vždy držala palce a motivovala ma k ďalšej práci. Vždy ste vo mňa verili a preto Vám ďakujem. Vďaka patrí aj mojim výnimočným priateľom, z ktorých by som sa osobitne chcela poďakovať Lukášovi, no najmä Karin. Boli pre mňa oporou vždy, keď som potrebovala. Všetkým ostatným, ktorí na mňa mysleli taktiež ďakujem.

Prohlášení

Prohlašuji, že jsem svoji bakalářskou práci vypracovala samostatně s využitím informačních zdrojů, které jsou v práci citovány.

Brno 24. května 2018

Podpis autora

Contents

Foreword

Since I was young I have been interested in the universe topic. This interest I share with my father who has brought me to this beautiful hobby. Since I was successfully accepted for the field of study I am studying now, I can fully devote myself to this fascination. Science is progressing faster and faster, however, there are still new hypotheses waiting for confirmation. Between many research objects I always choose topics such as dark matter or what is inside the black holes. That is why I have chosen the dark matter field for my Bachelor's thesis.

Of course, I am not trying to definitely prove of definitely disprove the hypothesis about existence of this interesting substance. Nonetheless, the quite simple simulations I have created could incline the reader's outlook to the way my results tend.

In this thesis I am mostly focusing on learning to work with simulation models, understanding the dark matter and galactic fields and improve my programming logic and skills. But the most important for me is to create a compact view of myself about this controversial topic based on my results.

Motivation

According to the studies we are encountering the missing mass problem. This issue can be solved by using two different concepts. The first is adjustment of classic physical equations using method called MOND. The second is acknowledging existence of a new substance, dark matter in Lambda-CDM model.

Which one of these theories is closer to the truth? If we assume that ΛCDM is the right model, will we be able to recognize changes in structure of shells in shell galaxies made by a sub-halo transit? If positive, are we really closer to the truth?

This is the motivation to the Interactions of dark matter and stellar halos in shell galaxies topic.

1 Introduction

In this section I am giving a brief introduction to galaxies, their classification and morphology. There are different types of galaxies. This difference came from their dissimilar formation mechanisms and time when they had formed.The source of this information comes from [1], [2] and [3]. After this short introduction to galaxy problem I am focusing on shell galaxies and their formation. as described in [4] and [5].

1.1 Galaxy formation

According to cosmological simulations galaxies started their formation about 13 billion years ago, which means about 700 million years after the Big Bang. Theories of galaxy formation is the relative importance of gravitational processes and of gas-dynamical effects. Many of the properties of galaxies indicate that there are mainly two types of galaxy formation.

Top-Down theories show that disk galaxies (the primordial shape) are formed through a collapse of a huge cloud of gas. This cloud is supposed to be bigger than the final galaxy. This scenario is based on the principle that radiation smoothed out the matter density fluctuations to produce large “pancakes”. These pancakes accrete matter after recombination and grow until they collapse and fragment into galaxies. This scenario predicts that there should be large sheets of galaxies with low density voids between the sheets. In regions where the sheets intersect clusters of galaxies are formed.

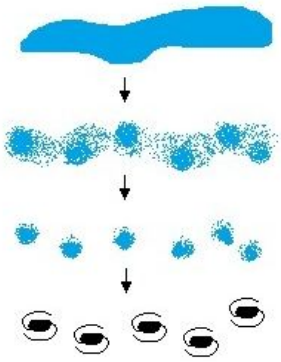

Figure 1.1: Top-Down Structure Formation. In this scenario, large "pancakes" are formed and than fragmented into galaxy-sized lumps.

The second theory of modeling disk galaxies is Bottom-Up Scenario. In this one galaxies form first and merge into cluster. At the time of recombination, the density enhancements are close to the size of small galaxies today. These enhancements collapse into dwarf galaxies from self gravity. Small galaxies attract each other by gravity and merge to form larger ones. Then they can form filaments and clusters.

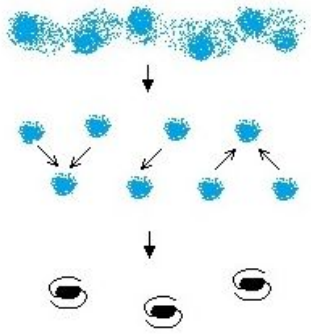

Figure 1.2: Bottom-Up Structure Scenario. In this scenario, dwarf galaxy-sized lumps are formed first, than merger to make galaxies and clusters of galaxies.

Best way to make simulations corresponding to the observations is combining both types of evolution of galaxy formation.

Figure 1.3: In the centre, in the darker cloud of gas, we can see a spectacular star-forming region known as the Flame Nebula. Credit: ESO/J. Emerson/VISTA. Acknowledgment: Cambridge Astronomical Survey Unit. Edited from [6].

1.2 Types of galaxies

Even early galactic astronomy divides galaxies into three groups: elliptical galaxies, spiral galaxies and irregular galaxies. These groups were first thought to be stages of galaxy evolution. However, later scientists showed that they all have same age, about 13 billion years. So as the differences are caused by different scenarii of evolution, but not the age. The brief overview of these three types is given below.

1.2.1 Elliptical galaxies

If the initial rotation of the galaxy is relatively low, the formation of stars begins earlier than the flattening of the disk. The flattening continues very rarely due to the small number of star collisions. This is the principle of an elliptical galaxy formation.

The shape of elliptical galaxies is a spheroid, or elongated sphere. The light is smooth, with the surface brightness decreasing as going further out from the centre. Ellipticals contain neither interstellar dust nor bright stars of spectral types O and B. Ellipticals are red in colour, and their spectra indicate that

their light comes mostly from old stars, especially evolved red giants. Elliptical galaxies have no particular axis of rotation.

Figure 1.4: The giant elliptical galaxy M87, also known as Virgo A, in an optical image taken by the Canada-France-Hawaii Telescope on Mauna Kea, Hawaii. M87 appears near the centre of the Virgo Cluster of galaxies. Credit: J.-C. Cuillandre and G. Anselmi—Canada-France-Hawaii Telescope(CFHT)/Coelum. Edited from [7].

1.2.2 Spiral galaxies

The faster the initial rotation, the bigger number of gas-clouds collisions. The flattening of the disk happens faster than the formation of the most of the stars and density waves are evolved.

The thicker parts shine more brightly and produce more stars that are formed here. These parts are called spiral arms and they are made up of dust and gas. Younger stars are formed here. On the other hand, the halo of the galaxy is a loose, spherical structure located around the central bulge and some of the arm structure. The halo contains old clusters of stars, known as globular clusters.

Figure 1.5: The Pinwheel Galaxy (M101), as seen in an optical image taken by the Hubble Space Telescope. Credit:NASA, ESA, CXC, SSC, and STScI. Edited from [8].

1.2.3 Irregular galaxies

Irregular galaxies have no definite structure. The stars are bunched up but the patches are randomly distributed throughout the galaxy. Most irregulars are small and faint. The dwarf irregulars may be the most common type of galaxy in the universe.

They are divided into two groups, Irr I and Irr II. Irr I type galaxies have regions of elementary hydrogen gas and many young hot stars. Irr II have large amounts of dust blocking most of the light from the stars which makes seeing distinct stars in the galaxy almost impossible.

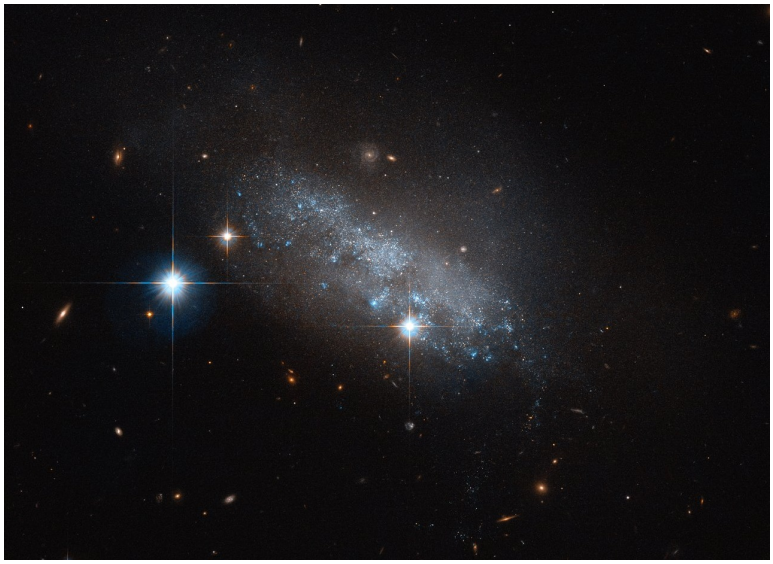

Figure 1.6: An irregular galaxy IC 3583 about 30 million light-years away in the constellation of Virgo. Credit: ESA/Hubble & NASA. Edited from [9].

1.3 Shell galaxies

Galaxies build up their stellar mass via star formation and successive mergers. Often times, these mergers leave behind unique morphological features in the extended stellar halos, such as stellar shells, rings or plumes of the galaxies. These features depend on the mass of merging objects.

The first shell galaxies were reported in the Atlas of Peculiar Galaxies created by Arp in 1966 [10]. It was the first catalogue of shell galaxies. For revealing shell structures the post-processing was used which resulted in the identification of 137 galaxies with shells by Malin and Carter in 1983 [11]. It was the first time the notion "shell" was used for these structures which were observed in Arp 230.

Early results suggest that shell-like structures are relatively common feature of massive elliptical galaxies with one or more shells observed. Recent studies show that 12 of 55 nearby elliptical galaxies exhibit shells. However, only 9 of 260 early-type galaxies occur to have these shell structures. Everything depends on the selection criteria.

Figure 1.7: Galaxy NGC 474 spans about 250,000 light years and lies about 100 million light years distant toward the constellation of the Fish (Pisces). Credit: P.-A. Duc (CEA, CFHT), Atlas 3D Collaboration, [12].

1.3.1 Shell-formation models

Theories invoked a varied range of mechanisms of creating shell structures. Most probably scenario is the merger scenario. In this scenario shells are supposed to be created by a merge of two different galaxies. Primary galaxy, the more massive one, is supposed to be merged by the lighter secondary galaxy by falling onto the centre of the primary one. The merger creates differences in the gravitational field of the primary galaxy. The shells are density waves made of the stars of the secondary galaxy (similar to waves on the water surface). The primary galaxy remains almost the same, while the secondary one's stars start orbiting the centre of the primary galaxy.

A competing theory is based on tidal interactions. It models shells as density waves induces in the cold disk by a passing galaxy. The problem is that elliptical galaxies are actually hot dynamic systems. However, these galaxies can have a thick disk with a number of cold stars which is not detected. In this model, shells are predicted to have similar colors to the host. Outer shells occur to be bluer than inner ones.

Analytical and numerical work supports the merger scenario. It would be good to note that the word "merge" doesn't actually mean the same as usual.

The distances between stars in galaxies are that large that there is almost no probability of a classical physical merge. In this case we mean merge as considerable gravitational interaction.

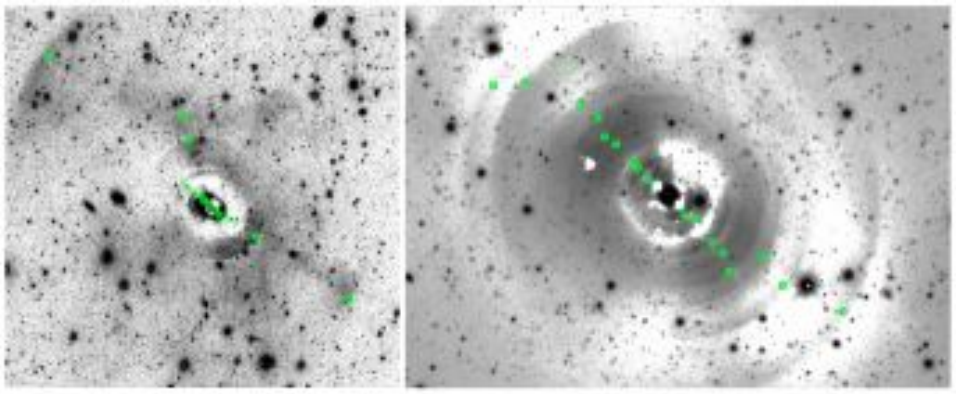

Figure 1.8: Galaxy NGC 3923. Green dots show counts of the shells of NGC 3923 simulated in Illustris simulation. Credit: Erwin, P. Imfit: A Fast, Flexible New Program for Astronomical Image Fitting, [13].

2 The missing mass problem

Physics of galaxies encounters the missing mass problem. According to General Relativity or Newtonian dynamics we should observe smaller gravitational interaction than we actually do. There are basically two possible theories solving this problem, the existence of so called dark matter and modifying some of the standard laws of physics. The source of information for this section is from [1], [14], [15], [16], [17], [18], [19] and [20].

2.1 Dark matter

Dark matter does not interact with electromagnetic force unlike normal matter. That means it does not emit, absorb or reflect light, which results in extremely hard optical detection. However, dark matter interacts with visible matter gravitationally. Dark matter candidates arise frequently in theories such as supersymmetry and extra dimensions. The first who attempted a dynamical estimate of the amount of dark matter in the Milky Way was Lord Kelvin. He established a relationship between the size of the system and the velocity dispersion of the stars in this system. However, he predicted more stars in the system than were actually observed. He claimed, that majority of stars may be dark bodies. Now it is calculated to be about 70 %. However it is quite demanding to posses its properties and include dark matter volumes into equations.

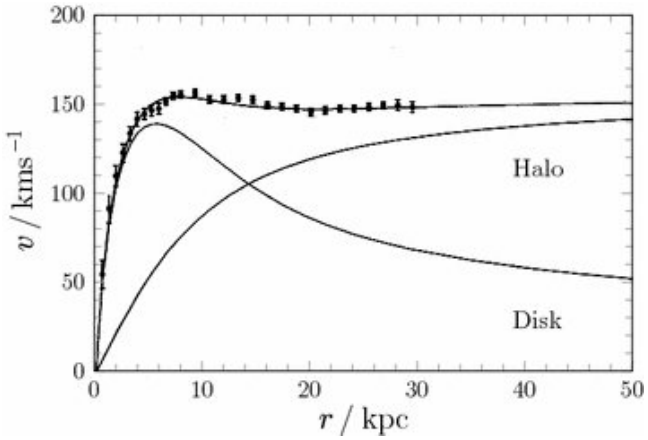

Figure 2.1: Orbiting material around the centre of a galaxy was measured by Doppler's effect. Luminous material seems to be concentrated towards the center and drops off with increasing distances, [16].

2.1.1 Dark matter halo

A dark matter halo is a hypothetical element of a galaxy surrounding the galactic disc. The total mass of the halo is larger than the mass of the visible matter however, it has never been observed directly. Dark matter halos play a big role in formation and evolution of galaxies.

During initial galactic formation, gravitationally self-bound objects could not have been formed of baryonic matter due to relatively high temperatures. For increasing the gravitational interactions, there is formation of dark matter structure assumed to be required. The hypothesis for this is based on the formation of cold dark matter into structure in the early universe. This hypothesis started when density perturbations in the universe had occurred. The perturbations increase linearly until reaching a critical density ρ_{crit} defined as

$$\rho_{\mathsf{crit}} = \frac{3H^2}{8\pi \mathsf{G}}, \tag{2.1}$$

where H is the Hubble parameter and G is the gravitational constant. After that they stop enlarging and collapse into dark matter halos. They then continue to grow in mass and size, even though they merge another object or a halo. Some halos are smaller, but that does not mean that this size is their final stage. They merge with each other to form a single dark matter halo which is assumed to have a substructure represented by sub-halos around the centre. They orbit within the potential well of their mother halo (host). While orbiting the sub-halo looses its weight due to strong tidal forces from the host. The sub-halo is then subjected to dynamical friction which is attended by energy and angular momentum loss in behalf of its mother halo. The lifetime of a sub-halo depends on its mass, orbit and density profile. For simplicity I am predicting no such losses in my simulations.

The cold dark matter (CDM) theory controls problems with the visible baryonic matter collapses triggered by the thermal and radiative pressures. The lower CDM temperatures in opposite to the baryonic matter temperatures allow the dark matter to form this substructure. As soon as the sub-halos are formed, their interaction with the visible baryonic matter overcomes the thermal energy and enables them to collapse into stars and other objects such as galaxies.

There are still uncertainties in both the data and the model assumptions about the exact shape type of the dark matter halos. The density profile of dark matter halos is predicted to be Navarro-Frenk-White (NFW) profile which I am discussing in 3.2.

2.2 Modified Newtonian dynamics

Modified Newtonian dynamics (MOND) is a theory in physics, that remodels standard Newton's laws to better fit observations and properties of galaxies. It was first published by M. Milgrom in 1982 [17]. He wanted to explain the missing mass problem with no need to assume hidden mass in significant quantities. Considering that Newton's second law does not describe the motion of objects in galaxies and galaxy systems. Using a more general function of acceleration of the object with assumptions leads to the form

$$m_{\mathsf{g}}\mu\Big(\frac{a}{a_0}\Big)\boldsymbol{a} = \boldsymbol{F}, \tag{2.2}$$

$$\mu(x \gg 1) \approx 1, \qquad \mu(x \ll 1) \approx x,$$

where m_{g} is the gravitational mass of a body moving with acceleration $\boldsymbol{a}$ ($a = |\boldsymbol{a}|$) moving in a arbitrary static force field $\boldsymbol{F}$, a_0 is an acceleration constant and $\mu(a/a_0)$ is and interpolating function. It can have two variations. The "simple μ-function"

$$\mu\Big(\frac{a}{a_0}\Big) = \frac{1}{1+\frac{a_0}{a}}, \tag{2.3}$$

and the "standard μ-function"

$$\mu\Big(\frac{a}{a_0}\Big) = \frac{1}{\sqrt{1+\big(\frac{a_0}{a}\big)^2}}. \tag{2.4}$$

For accelerations $a \gg a_0$ is $\mu(x \gg 1) \approx 1$ and Newtonian dynamics is restored. In the limit of small accelerations $a \ll a_0$, the acceleration of the particle satisfies approximately

$$\frac{a^2}{a_0} \approx \frac{\mathsf{G}M}{r^2}, \tag{2.5}$$

where r is the distance of the particle from a mass M.

Applying these equations to a body with mass orbiting around a point mass M circularly, we get

$$\frac{\mathsf{G}M}{r^2} = m\frac{a^2}{a_0} = \frac{mv^4}{r^2 a_0} \quad \longrightarrow \quad v = \sqrt[4]{\mathsf{G}Ma_0}. \tag{2.6}$$

Equation (2.6) explains almost constant radial velocities of stars further from the center.

This theory found by Milgram is not complete, however it provides a concise description of observational facts. The alternative to this theory is ΛCDM model assuming the existence of dark matter.

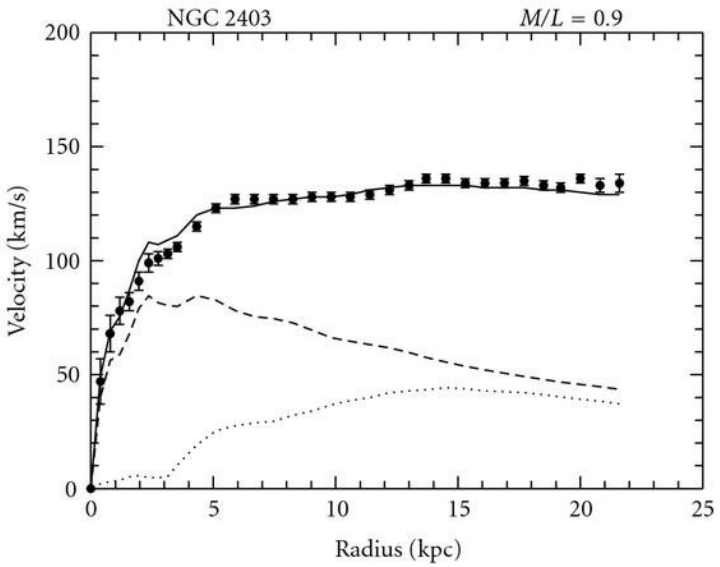

Figure 2.2: The 21 cm line rotation curve of NGC 2403 almost perfectly fallows the MOND (solid) curve. The dashed curve represents the Newtonian rotation curve of the visible disk (assuming a constant mass-to-light ratio of 0.9 in solar units), and the dotted curve captures the Newtonian rotation curve due to the gaseous component (H, He), [21].

2.3 Lambda-CDM model

The ΛCDM model or Lambda cold dark matter model is a parametrization of the cosmological model of Big Bang. In this model universe contains a cosmological constant represented by Λ and the cold dark matter (CDM). The ΛCDM includes the expansion of cosmos which is documented as the red shift of distant galaxies' spectral lines and also as the time dilation in the light decay of supernova luminosity curves. Both of these effects are results of Doppler's effect.

The cosmological constant Ω_Λ relates to the dark energy of vacuum. Pressure of the cosmological constant, contributing to the stress-energy tensor, is

$$p = -\rho c^2, \tag{2.7}$$

which explains the accelerating expansion phenomenon working opposite to the gravitational effect. The fraction of the total mass density and energy of flat universe is represented by Ω_Λ. Planck satellite data in 2015 estimated Ω_Λ to be 0.6911 ± 0.0062.

Cold dark matter consists of matter other than baryons or electrons. The word "cold" represents the velocity of CDM $v_{\text{CDM}} \ll c$ at the epoch of radiation-matter equality, where c is the speed of light.

In my simulations I am going to test the ΛCDM model on built in galaxies and try to prove its relevance on simplified situations.

3 Density distribution models

The dynamical theory of stellar systems is used to determine the masses of galaxies and systems of galaxies. When talking about stellar systems we mean self-gravitating point masses, which may be stars or galaxies. We are going to use spherical symmetry because most of the objects we will be using have spherical potential distribution, although they seem to be flattened. In general the distribution functions for real stellar systems are not known. However, using analytic distribution can be used to describe such functions. Below I am giving two of the most common models of potential distribution as described in [22], [23] and [24].

3.1 Plummer model

The Plummer model is one of the simplest models of stellar systems. To represent the observed density profiles of star clusters is the Plummer model often used and fits well with the observations at relatively small radii.

The power-law for the phase space distribution function is given as

$$f(E, L^2) = \begin{cases} K\,|E|^{\frac{7}{2}} & \text{for } E < 0 \\ 0 & \text{for } E > 0. \end{cases} \tag{3.1}$$

In this case, the density distribution becomes

$$\rho(r) = 4\pi K \int_0^{\sqrt{2}|\phi|} \left(|\phi| - \frac{1}{2}v^2 \right)^{\frac{7}{2}} v^2 \mathrm{d}v = 7\pi^2 \cdot 2^{\frac{-11}{2}} K\,|\phi|^5 \,. \tag{3.2}$$

Let's assume that $\rho(r)$ satisfies Poisson's equation

$$\frac{1}{r^2}\frac{\mathrm{d}}{\mathrm{d}r}\left(\frac{r^2|\phi|}{\mathrm{d}r}\right) = -4\pi \mathsf{G}\rho = -4\pi \mathsf{G} \cdot 7\pi^2 \cdot 2^{\frac{-11}{2}} K\,|\phi|^5 \,. \tag{3.3}$$

A solution is the potential form

$$\Phi_{\mathsf{P}}(r) = -\frac{\Phi_0}{\sqrt{1 + \left(\frac{r}{r_{\mathsf{P}}}\right)^2}}, \tag{3.4}$$

where Φ_0 is the central potential and r_{P} is the characteristic length scale

$$r_{\mathsf{P}}^2 = \frac{3 \cdot 2^{\frac{7}{2}}}{7\pi^3 \mathsf{G} K\, \Phi_0^4}. \tag{3.5}$$

The density distribution extends to infinity, but the mass distribution is finite. However, the density fall-off at large radii ($\rho(r) \to r^{-5}$) does not fit the observations. The observed brightness density decays more slowly (r^3 to r^4). We see that using this quite simple model at small radii, as I will be using in my simulations for galaxies, gives good results.

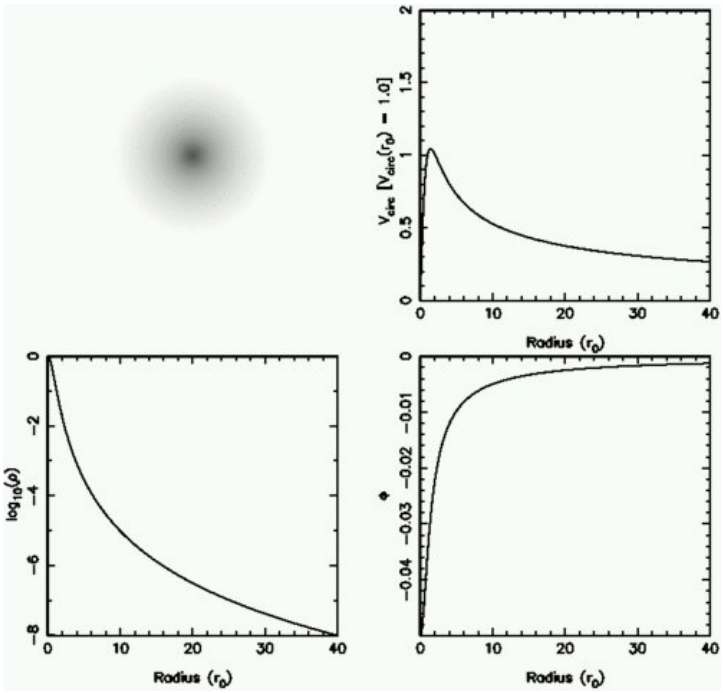

Figure 3.1: These plots show an image of density distribution of Plummer's model, along with the generating potential and the circular velocity as a function of distance from the center, [25].

3.2 Navarro–Frenk–White model

The Navarro–Frenk–White model or NFW model is often used to model a spatial mass distribution of dark matter halos identified in N-body simulations by Navarro, Frenk and White in 1996 [24]. It is an approximation to the equilibrium configuration of dark matter. Analytic calculations and numerical simulations both suggest that the density profiles of dark matter halos may contain practical information concerning the cosmological parameter of the universe.

Density fluctuations are well fitted by the formula

$$\rho(r) = \frac{\rho_{\mathsf{c}}^0}{\left(\frac{r}{r_{\mathsf{NFW}}}\right)\left(1+\frac{r}{r_{\mathsf{NFW}}}\right)^2}, \tag{3.6}$$

where ρ_{c}^0 is the critical density, r_{NFW} is the scale radius, c represents the concentration parameter which is related to the scale radius by

$$r_{\mathsf{NFW}} = \frac{r_{\mathsf{v}}}{c}, \tag{3.7}$$

where r_{v} is the virial radius. All these parameters vary from halo to halo and represent the specific mass distribution.

The mass of and object we get by integrating the specific density profile within some volume as

$$\begin{aligned} M(r) &= \int_0^{2\pi}\int_0^{\pi}\int_0^{R} r^2 \sin\vartheta\rho(r)\mathsf{d}\varphi\mathsf{d}\vartheta\mathsf{d}r \\ M(r) &= 4\pi\rho_{\mathsf{c}}^0 r_{\mathsf{NFW}}^3\Big[\ln\frac{r_{\mathsf{NFW}}+R}{r_{\mathsf{NFW}}} - \frac{R}{r_{\mathsf{NFW}}+R}\Big]. \end{aligned} \tag{3.8}$$

Using the concentration parameter c we get the total mass of the object given as

$$M(c) = 4\pi\rho_{\mathsf{c}}^0 r_{\mathsf{NFW}}^3\Big[\ln(1+c) - \frac{c}{1+c}\Big], \tag{3.9}$$

where c usually varies from 4 to 40 for various halos. As we can see, the mass would go to infinity for $r \to \infty$, that is why we integrate within the volume where the gravitational interaction with the environment is significant.

The gravitational potential $\Phi_{\mathsf{NFW}}(r)$ of this mass is simply given by integrating

$$\Phi_{\mathsf{NFW}}(r) = \int_R^{\infty} \frac{-\mathsf{G}M(r)}{r^2}\mathsf{d}r. \tag{3.10}$$

For the NFW potential we get

$$\Phi_{\mathsf{NFW}}(r) = -4\pi\mathsf{G}\rho_{\mathsf{c}}^0 r_{\mathsf{s}}^3\frac{\ln\left(1+\frac{R}{r_{\mathsf{s}}}\right)}{R}. \tag{3.11}$$

According to assumptions that the dark matter forms about 70 % of the universe we can use the NFW profile not only for dark matter halos but also for whole galaxies. That is why I am going to use the NFW profile for galaxies in my simulations as well.

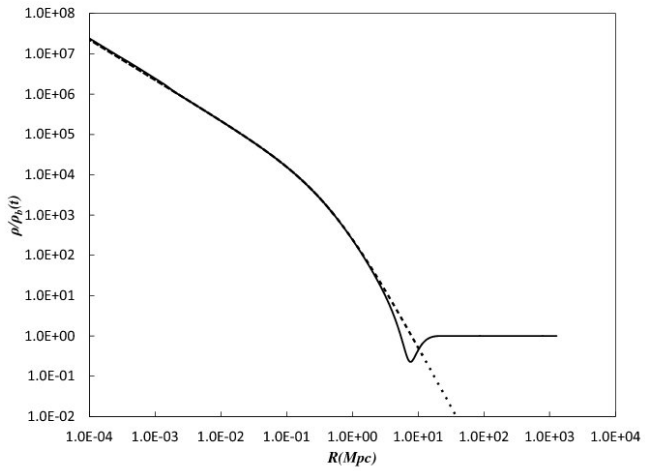

Figure 3.2: Density profile for a cluster. Dot line is for original NFW profile and solid line is the LTB model (NFW near center that tends to background density via a compensated underdensity), [26].

4 Motion in a gravitational field

According to Newton's first law of motion, there must be an imbalance of all existing forces acting upon an object to be in motion with a velocity which is not constant. Newton's second law of motion explains this. It states that the acceleration of an object is dependent upon two variables - the net force acting upon the object and the mass of the object. This relation is linear dependent, written as

$$\boldsymbol{F} = m\boldsymbol{a}. \tag{4.1}$$

The force can also be related to some classical field, for example a gravitational one. If we are contemplating a position in the field, for this position we can describe the force acting in this position simply by the negative gradient of the potential of the field in this position. The minus sign describes the opposite direction of the force vector over the gradient of the potential written as

$$\boldsymbol{F} = -\nabla \Phi(r). \tag{4.2}$$

We contemplate only gravitational effects. Effects such as electromagnetic or nuclear ones can be neglected because of the large relative distances which lead to tiny actions caused by these other types of field. Knowing the mass of an object we get the acceleration given by the gravitational field. In my simulations we are using the NFW potential for the primary galaxy and the sub-halo of dark matter and the Plummer potential for the secondary galaxy (before the merger). The following differential equations can be solved only numerically. For the NFW potential from (3.11) we get the acceleration

$$\boldsymbol{a}_{\mathsf{NFW}} = -4\pi \mathsf{G}\rho_{\mathsf{c}}^{0} r_{\mathsf{NFW}}^{3} \frac{\left[\frac{r_{\mathsf{NFW}} \ln(1+r/r_{\mathsf{NFW}})}{r} + \ln\left(1 + r/r_{\mathsf{NFW}}\right) - 1\right]}{r^2\left(r + r_{\mathsf{NFW}}\right)} \boldsymbol{r}, \tag{4.3}$$

and for the Plummer potential we get

$$\boldsymbol{a}_{\mathsf{P}} = -\frac{\mathsf{G}M}{\left(r^2 + r_{\mathsf{P}}^2\right)^{\frac{3}{2}}} \boldsymbol{r}. \tag{4.4}$$

The objects moving with accelerations described above will be the secondary galaxy first and then the sub-halo. The secondary galaxy is represented by a number of point particles deployed according to Plummer potential and not interacting with each other. The sub-halo is represented only by NFW potential but no point particles, because we want to see the effect of the sub-halo on the

shells which are created by the point particles of the secondary after the merger of these two galaxies, primary and secondary.

4.1 Leapfrog

As I mentioned above, the differential equations describing acceleration of an object for both, NFW and Plummer potential can be solved only numerically. We can use leapfrog integration method to solve this problem. In this algorithm positions and velocities 'leap over' each other. Positions are defined at times t_i, t_{i+1}, t_{i+2},..., spaced at constant intervals $\mathrm{d}t$. The velocities are defined at times halfway in between, indicated by $t_{i-1/2}, t_{i+1/2}, t_{i+3/2}$,..., where $t_{i+1} - t_{i+1/2} = t_{i+1/2} - t_i = \mathrm{d}t/2$. Then the leapfrog integration scheme is

$$\boldsymbol{r}_i = \boldsymbol{r}_{i-1} + \boldsymbol{v}_{i-1/2}\mathrm{d}t, \tag{4.5}$$

$$\boldsymbol{v}_{i+1/2} = \boldsymbol{v}_{i-1/2} + \boldsymbol{a}_i\mathrm{d}t. \tag{4.6}$$

As we can see, the accelerations $\boldsymbol{a}$ and the positions $\boldsymbol{r}$ are defined only on integer times, while the velocities $\boldsymbol{v}$ are defined only on half-integer times. This means that the acceleration of one particle depends only on its position in space.

At the beginning of the integration we have to set up the velocity at its first half-integer time step. We also have to set up initial conditions of the position $\boldsymbol{r}_0$ and velocity $\boldsymbol{v}_0$. Then we use the Taylor series expansion to compute the first leap value for the velocity

$$\boldsymbol{v}_{1/2} = \boldsymbol{v}_0 + \boldsymbol{a}_0\mathrm{d}t/2. \tag{4.7}$$

Now we can compute the new position $\boldsymbol{r}_1$ using the first leap value $\boldsymbol{v}_{1/2}$ by applying (4.5) and (4.6). Next we are able to compute the acceleration $\boldsymbol{a}_1$, which enables us to compute the second leap value, $\boldsymbol{v}_{3/2}$, using (4.7), and so on.

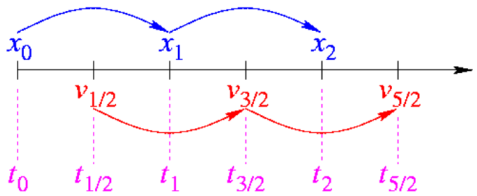

Figure 4.1: Leapfrog method scheme, [27]

Such an algorithm I am using in my simulations. The source of the information is from [28].

5 Introduction to the simulation model

5.1 The Merger

5.1.1 Galaxies as merger objects

As I am focusing on simulating transit of a dark matter sub-halo through a shell galaxy in my Bachelor's thesis, I have to create such a shell galaxy first. As I mentioned in the first section, shell galaxies are usually created by a merger of two galaxies. For my simulation I chose a merger of a typical elliptical galaxy representing the primary galaxy with mass $M_{\mathsf{p}} = 3.2 \cdot 10^{11}$ $\mathsf{M}_{\odot}$ and scale radius $r_{\mathsf{NFWp}} = 5$ kpc. This scale radius we have computed providing that the primary galaxy is represented by NFW potential. For such a type of potential is one more independent parameter needed, which is the density ρ^0_{cp}. We have also computed using equations for NFW potential and we get $\rho^0_{\mathsf{cp}} = 6.63 \cdot 10^{-21}$ $\mathsf{kg} \cdot \mathsf{m}^{-3}$.

The secondary galaxy (the merging object) we set to be a dwarf elliptical galaxy with mass of 1 % of the primary one. We followed the original selection of the galaxies made by Dr Bruno Jungwiert and edited by Vaclav Glos [29]. The scale radius of this secondary galaxy is then 10 % of the primary one, which is $r_{\mathsf{Ps}} = 0.5$ kpc. This value we got assuming that the mass of the secondary is $M_{\mathsf{s}} = 3.2 \cdot 10^9$ $\mathsf{M}_{\odot}$ and was computed using equations for the Plummer potential we want the secondary galaxy to have. For the Plummer potential depiction we also have two independent parameters, the mass and the scale radius r_{Ps}. We already have both of these parameters.

Setting the independent parameters using equations representing both potentials to describe galaxies we managed to use is not really outright. However, small deviation values (by maximum of 10 %) should not play a big role in the shell creation.

As we want to observe the shell formation after the merger which are created by particles of the secondary galaxy, we set the secondary represented by a number of non-interacting particles in Plummer potential. Efficient setting of the particle number affects the accuracy of results but also the speed of the simulation computing. That is why chose the number of secondary particles to be $\mathsf{N_s} = 10^6$ particles. We also let the primary galaxy to be represented only by the NFW potential (with no particles) to observe only formed shells in resolution.

5.1.2 The initial positions and velocities of the galaxies

In this moment we can set the initial conditions of positions and velocities of our galaxies according to the Leapfrog method. For simplicity we chose the origin of coordinate system to be in the centre of gravity of the system. We

also let the galaxies move only along the x axis. That means we only have to set the initial relative distance of the objects customized to fit the centre of gravity position. We set this distance to be $d = 91.2$ kpc. The initial position of the primary galaxy according to the ratio of masses will be a lot closer to the centre than the secondary ones. The initial position of the primary we set to $\boldsymbol{r}_{\mathsf{p}} = (-0.9, 0, 0)$ kpc. The initial position of the secondary we easily get from the relative distance and the initial position of the primary and we get $\boldsymbol{r}_{\mathsf{s}} = (90.3, 0, 0)$ kpc.

For the motion along the x axis we also need to set initial velocities. For the initial velocity of the secondary we chose the x component of the initial velocity to be 99 % of the escape speed of the secondary to get as effective results as possible. The initial velocity of the secondary is then $\boldsymbol{v}_{\mathsf{s}} = (-0.99 v_{\mathsf{esc}}, 0, 0)$, where v_{esc} is

$$v_{\mathsf{esc}} = \sqrt{\frac{2(M_{\mathsf{p}} + M_{\mathsf{s}})}{\sqrt{d^2 + \delta^2}}} \tag{5.1}$$

and δ is softening distance. As the primary galaxy is not in the centre of the coordinate system, we get the components of its velocity according to the mass ratio as $\boldsymbol{v}_{\mathsf{p}} = -0.01 \boldsymbol{v}_{\mathsf{s}}$. Then we can set the initial velocity of the primary galaxy to be $\boldsymbol{v}_{\mathsf{p}} = (-0.01 v_{\mathsf{sx}}, 0, 0)$. After the merger of our galaxies we switch off the secondary potential and give the primary zero speed. Now we can run the merger and the shell formation simulation.

5.2 The sub-halo transit

After the merger simulation we are going to model a transit of a dark matter sub-halo through our new shell galaxy. For the sub-halo we also need to set initial parameters. Assuming that the sub-halo has NFW profile, we need to choose suitable parameters. I decided to simulate transits of sub-halo of three different masses which are 10^9 $\mathsf{M}_\odot$, 10^8 $\mathsf{M}_\odot$ and 10^7 $\mathsf{M}_\odot$. For every mass there are different parameter values, so I decided to put them in Table 5.1 below for a better overview.

The same as for the primary galaxy we assume zero number of the particles for the sub-halo.

5.2.1 The initial positions and velocities of the sub-halo

The initial position of the sub-halos I set to be the same. The sub-halo is gravitationally bound to this primary galaxy and also must be able to move through the created shells of it. I set this distance to be 100 kpc. The position in the coordinate system will now be represented by non-zero components for more

$M[\mathrm{M}_\odot]$	$\rho_\mathrm{c}^0 \cdot 10^{-21}[\mathrm{kg} \cdot \mathrm{m}^{-3}]$	$r_\mathrm{NFW} \cdot 10^{-2}[\mathrm{kpc}]$
10^9	1.93	13.2
10^8	3.36	6.1
10^7	5.90	2.8

Table 5.1: Parameters of the NFW potential set for different masses of the sub-halo

realistic example. The z coordinate I put 10° above the xy level, the y coordinate is 60° tilted from the y axis and the x coordinate is 30° tilted from the x axis. The initial position of the sub-halo is then $\boldsymbol{r}_\mathrm{h} = (853, 492, 174) \cdot 10^{-1}$ kpc.

The initial velocities of the sub-halos I decided to set as the sub-halos are gravitationally bounded to the primary and orbiting around the centre of it in two real different speeds. The difference between them is 10 %. For a better overview I am depicting these two vectors of velocities in Table 5.2:

	$v_\mathrm{hx}[\mathrm{km} \cdot \mathrm{s}^{-1}]$	$v_\mathrm{hy}[\mathrm{km} \cdot \mathrm{s}^{-1}]$	$v_\mathrm{hz}[\mathrm{km} \cdot \mathrm{s}^{-1}]$
Type 1	- 55.4	- 9.6	- 19.5
Type 2	- 61.6	- 10.7	- 21.7

Table 5.2: Components of the two types of the sub-halo velocity

For a better depiction I edited my simulation model to generate positions of the sub-halo during 100 Gyr with mass 10^9 $\mathrm{M}_\odot$. I have set such a wide time scale to show the periodicity of motion. In a picture below I am showing the two types of trajectories of the sub-halo described in Table 5.2.

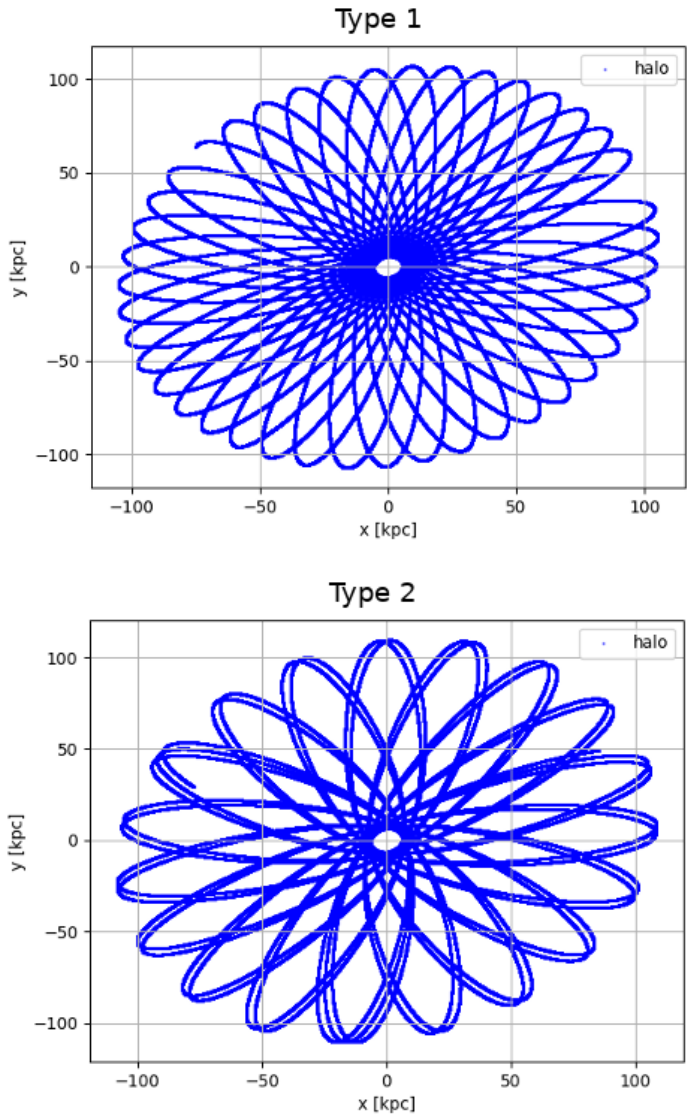

Figure 5.1: The two types of sub-halo trajectories in the primary's potential during 100 Gyr with mass 10^9 $M_\odot$

I do not assume any changes in the position of the primary galaxy due to the symmetry of a number of sub-halo configuration around the primary. In this moment we can run our models and compare the results.

6 Simulation results

After my simulation model had finished I could compare the results. At first I would like to show what are the positions of shells and the sub-halo in xy plane and in zy plane at specific times for each type of the sub-halo velocity. I chose moments when the sub-halo was just after crossing a shell. In both cases the sub-halo is arriving at the shell perpendicularly from the outside.

6.1 Type 1 velocity

For the Type 1 velocity this time is 2.925 Gyr from the beginning of the simulation shown in Figure 6.1.

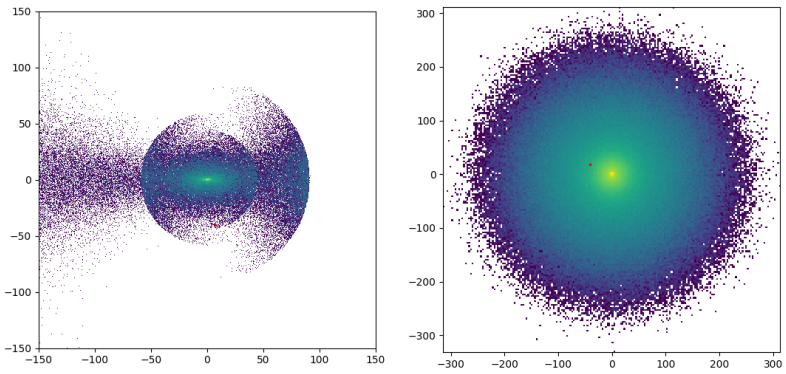

Figure 6.1: Type 1: Actual positions of the shells (blue and green) and the sub-halo (red) at 2.925 Gyr after the beginning of the simulation. Projection of the positions into xy plane is on the left and projection into yz plane is on the right.

The positions of all the three samples of the sub-halo masses are the same. However, the differences in shell shapes are expected. For a better overview zooming the graph of positions in xy plane is needed. In Figure 6.2 I am comparing the projection of the shell positions into xy plane for all three samples of the sub-halo mass and the shell position with no sub-halo included.

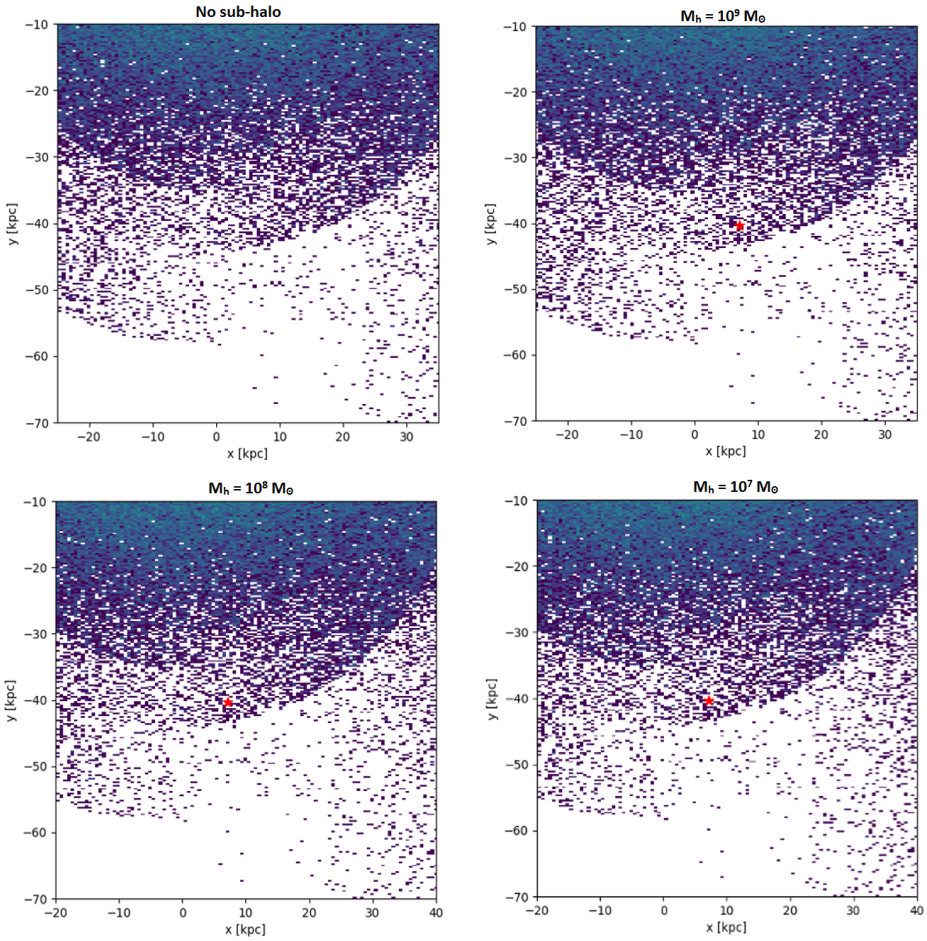

Figure 6.2: Type 1: Comparison of the actual positions of the shells at 2.925 Gyr projected into xy plane for different samples of sub-halo masses: no sub-halo (upper left), sub-halo mass of 10^9 $M_\odot$ (upper right), 10^8 $M_\odot$ (lower left) and 10^7 $M_\odot$ (lower right).

As we can see, there are no visible changes in shell distribution for any sub-halo mass sample moving in Type 1 velocity.

6.2 Type 2 velocity

For the Type 2 velocity the time just after the transit is 3 Gyr from the beginning of the simulation. Actual positions of the shells and the sub-halo are depicted in Figure 6.3.

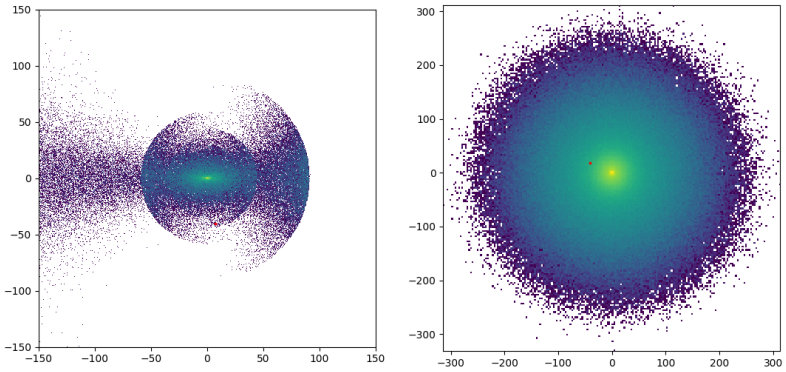

Figure 6.3: Type 2: Actual positions of the shells (blue and green) and the sub-halo (red) at 3 Gyr after the beginning of the simulation. Projection of the positions into xy plane is on the left and projection into yz plane is on the right.

To be able to see any visual differences in the shell distribution I am giving the comparison for the Type 2 in Figure 6.4. Type 2 speed is higher so there is a bigger probability to observe some kind of a shell displacement.

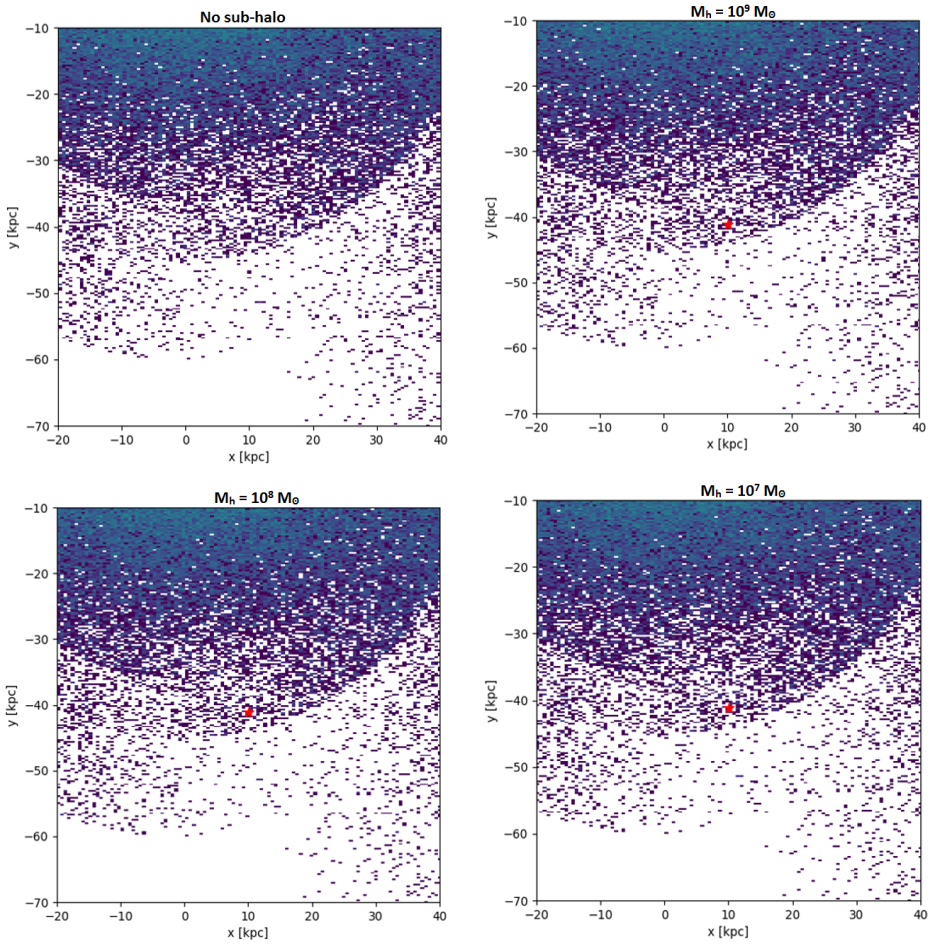

Figure 6.4: Type 2: Comparison of the actual positions of the shells at 3 Gyr projected into xy plane for different samples of sub-halo masses: no sub-halo (upper left), sub-halo mass of 10^9 $M_\odot$ (upper right), 10^8 $M_\odot$ (lower left) and 10^7 $M_\odot$ (lower right).

After a closer look at the shell distribution we can not see any changes in the shell distribution after the sub-halo transit for the Type 2 velocity.

6.3 Discussion

As I have mentioned in section 2, there are two theories explaining the missing mass problem, MOND and the ΛCDM model. MOND in opposite to ΛCDM does not permit existence of dark matter. Based on my results we have not observed any changes in the shell distribution after any of the sub-halo transits. After looking at images of real shell galaxies we also do not observe any changes and shells look uniform. As we were assuming the existence of dark matter because we were using a sub-halo as a test particle and it has not displayed any changes, I would consider these results to strengthen the dark matter idea, therefore, the ΛCDM model.

Conclusion

The first aim of this thesis was to look deeper into the dark matter and galaxy topic. Thanks to many publications related to these topics I have managed to find and read, my knowledge in this field has enriched enormously. As majority of them is written in English and also my decision to write my thesis in this language, I have improved my language skills and gained self-confidence for using English more often in the future.

The second of the aims was for me to familiarize myself with working with programming languages such as Fortran and improve my skills in using Python and LaTex. As I had to understand the original program to be able to edit it correctly, I consider learning to work with Fortran to be successful. Before this experience I had been afraid of programming, but after spending a lot of time doing it almost all the fear has disappeared. This I consider to be a huge personal success while working on this thesis.

The most important aim of my work was to create and compile simulations of different samples of sub-halos transiting a shell in a shell galaxy. Until the last moment when I have plotted zoomed graphs of shell and sub-halo positions and compared them with the original graph I had been impatiently awaiting to see the results. The existence of dark matter topic has been interesting for me since the first moment. The results of my work definitely do not disprove its possible existence what I have been hoping for. An idea of something that humanity has just started to understand has motivated me to work on it in my Bachelor's thesis. I am very satisfied that I could have contributed to this new topic. My personal view has strengthen thanks to my results. This is why I consider this aim fulfilled, too.

Appendices

In this section I have decided to append files and programs I had been using for my thesis. For example if someone decides to use them to compile their own simulations. These programs was not easy to work with in the beginning at all. However, later I have learned it at least a little. Because these programs are made to be used on computers I am appending them this way, not printed.

These programs are not the ones that majority of people usually already have in their computers. They are needed to be installed to compile the simulations. I personally prefer working with Linux operating system for such a computing work. Of course, I had to get used to this system. I have to admit that installing some programs was not that easy. However, these difficulties can be solved by finding a detailed installing process on the Internet. After a little while I learned working with these programs on my own and I am not afraid of working with Linux anymore.

In the following subsections I am describing and appending programs I have been using for my thesis.

I. The original simulation programs

The original program for simulating a shell galaxy formation [A1] has been created by my supervisor, RNDr. Bruno Jungwiert, Ph.D. It simulates a merger of two galaxies both having either Plummer sphere (described in 3.1) or de Vaucouleurs potential. These parameters were changed by Mgr. Václav Glos [A2] in his Bachelor's thesis. He made the primary galaxy have NFW density profile. As original and comparing simulation I am using outputs from the edited simulation model by Mgr. Glos.

Both these simulation scripts are written in a programming language called Fortran. Despite of its age it is more sufficient than other modern programs because of its computing speed. Of course, we need to install it. For Linux operating system there is a specific variant of Fortran called GNU Fortran. This installation is quite simple and quick. If there are any problems installing it I recommend an Internet search for the specific type of operation system you are using.

Along with Fortran there is also PG Plot needed to be installed. PG Plot, as seen in its name, plots graphs made in the simulations. The installation process is quite difficult so I am appending an Internet source with a detailed demonstration [A3].

To compile the simulations, there are two other files needed (merge.inp [A4] and young1976.dat [A5]) which are called in the script.

II. The individual sub-halo motion

To simulate the individual motion of the sub-halo I have edited the original model so it outputs a text file containing a table of the sub-halo positions in time [A6] for Type 1 velocity and [A7] for Type 2 velocity. As the real time I have used 1 Tyr to see the periodicity of the sub-halo and also its individual movement for both types of velocities. I remind that there must be both of the called files (merge.inp [A4] and young1976.dat [A5]) included in the folder where the script is saved. This simulation lasts only a few seconds.

After the simulation had finished, I have created a simple program in Python to plot the actual positions of the sub-halo in time [A8]. There also must be packages installed for Python. I am using Matplotlib and Numpy. It is very easy to install them so I am not adding their installation as an appendix.

III. Modeling the sub-halo transit

For the simulations I have been creating and evaluating in my thesis I have edited the original models. My personal experience is that editing the scripts in a text editor is the best. At first, I had been using the 'nano' command in Terminal, but there were a lot of errors when I was trying to compile the simulation. I have been editing the original file as I simulated an another particle (sub-halo) according to the assumptions described in 5.2. This sub-halo is moving in the potential of the primary galaxy, has its own density profile and has initial positions and velocities set for the Leapfrog computing method.

For every type of a sub-halo I had to create a specific model. I am appending all the 6 scripts. The names of the simulation models ended with 9, 8 and 7 sign the mass order in stellar masses. Number 1 and 2 sign the velocity type. I am giving the scripts of the velocity type 1 here [A9], [A10], [A11] and for the second velocity type here [A12], [A13], [A14].

The computing process lasts a longer time and the outputs are huge files of about 35 GB. My old notebook was computing one simulation for 13 hours, however, a powerful computer can make it about four times faster. That is why I recommend having enough time and disk space.

IV. Plotting the simulation outputs

An output of the simulation is a text file containing a table of the order number of a particle and its position in Cartesian coordinate system. Creating the output is edited to save only every 100^{th} step of a particle position and every step of the sub-halo position. If there was every single step saved to the output, the final file would not have the size of 35 GB but somehow about a few TB.

From these outputs I have also created graphs of positions in Python. To make a graph of the original file output without a sub-halo I have used a script [A15] created by Mgr. Glos. This script I have edited to show also the sub-halo position in a particular time. I am appending only 2 of these 6 scripts, because the halo position remains the same for the particular velocity. The only thing varying in these scripts are the opened (called) files [A16] and [A17]. For zooming the graph there is just changing the plotted scale needed for a suitable interval.

Appendix references

[A1] https://is.muni.cz/auth/th/fylur/prilohy/i/merger09.f?studium=727623.

[A2] https://is.muni.cz/auth/th/fylur/prilohy/i/mergerS_NFW.f?studium=727623.

[A3] https://guaix.fis.ucm.es/~ncl/howto/howto-pgplot.

[A4] https://is.muni.cz/auth/th/fylur/prilohy/i/merge.inp?studium=727623.

[A5] https://is.muni.cz/auth/th/fylur/prilohy/i/young1976.dat?studium=727623.

[A6] https://is.muni.cz/auth/th/fylur/prilohy/ii/merger_halo1.f?studium=727623.

[A7] https://is.muni.cz/auth/th/fylur/prilohy/ii/merger_halo2.f?studium=727623.

[A8] https://is.muni.cz/auth/th/fylur/prilohy/ii/halo1.py?studium=727623.

[A9] https://is.muni.cz/auth/th/fylur/prilohy/iii/merger_91.f?studium=727623.

[A10] https://is.muni.cz/auth/th/fylur/prilohy/iii/merger_81.f?studium=727623.

[A11] https://is.muni.cz/auth/th/fylur/prilohy/iii/merger_71.f?studium=727623.

[A12] https://is.muni.cz/auth/th/fylur/prilohy/iii/merger_92.f?studium=727623.

[A13] https://is.muni.cz/auth/th/fylur/prilohy/iii/merger_82.f?studium=727623.

[A14] https://is.muni.cz/auth/th/fylur/prilohy/iii/merger_72.f?studium=727623.

[A15] https://is.muni.cz/auth/th/fylur/prilohy/iv/singl_slupky_mil.py?studium=727623.

[A16] https://is.muni.cz/auth/th/fylur/prilohy/iv/single91.py?studium=727623.

[A17] https://is.muni.cz/auth/th/fylur/prilohy/iv/single92.py?studium=727623.

References

[1] White S. Mo H., Van den Bosch F. *Galaxy formation and evolution*. Cambridge University Press, 2010. ISBN 978-0-521-85793-2.

[2] Merrifield M. Binney J. *Galactic astronomy*. Princeton University Press, 1998. ISBN 0-691-02565-7.

[3] Guzman R. Galaxy formation and evolution." grandfather paradox. `https://www.astro.ufl.edu/~guzman/ast1002/class_notes/Ch15/Ch15b.html`, March 2018.

[4] Ebrova I. Shell galaxies: kinematical signature of shells, satellite galaxy disruption and dynamical friction, 2013. arXiv:1312.1643.

[5] Dobešová A. Poruchy v rotačních křivkách slupkových galaxií. Master's thesis, Masarykova univerzita, Přírodovědecká fakulta, Brno, 2017.

[6] The hidden fires of the flame nebula*. `https://www.eso.org/public/images/eso0949a/`, 2009. ESO.

[7] The giant elliptical galaxy messier 87. `http://www.cfht.hawaii.edu/HawaiianStarlight/HawaiianStarlight.html`, 2004. Image processing filters.

[8] Hubble image of m101. `https://www.spacetelescope.org/images/opo0907h/`, 2009. ESA/Hubble | ESA/Hubble.

[9] Spotlight on ic 3583. `https://www.spacetelescope.org/images/potw1648a/`, 2016. ESA/Hubble | ESA/Hubble.

[10] Arp H. Atlas of peculiar galaxies. *The Astrophysical Journal Supplement Series*, 14:1, 1966.

[11] Carter D. Malin D. A catalog of elliptical galaxies with shells. *The Astrophysical Journal*, 274:534–540, 1983.

[12] Bonnell J. Nemiroff R. Galaxy ngc 474: Shells and star streams. `https://apod.nasa.gov/apod/ap140105.html`, 2014. NASA.

[13] Puzia T. et al. Miller B., Ahumada T. The extended baryonic halo of ngc 3923. `http://www.mdpi.com/2075-4434/5/3/29/htm`, 2017. MDPI.

[14] Annika H. G. P. Dark matter: A brief review, 2012. arXiv:1201.3942.

[15] Hooper D. Bertone G. A history of dark matter, 2016. arXiv:1605.04909.

[16] Kluck H. *Production Yield of Muon-Induced Neutrons in Lead: Measured at the Modane Underground Laboratory (Springer Theses)*. Springer, 2015. ISBN 3319185268.

[17] Milgrom M. A modification of the newtonian dynamics as a possible alternative to the hidden mass hypothesis. *The Astrophysical Journal*, 270:365–370, 1983.

[18] de Blok WJG Gentile G., Famaey B. Things about mond. *Astronomy & Astrophysics*, 527:A76, 2011.

[19] Huterer D. Frieman J., Turner M. Dark energy and the accelerating universe. 2008.

[20] Carlisle C. Planck upholds standard cosmology. `http://www.skyandtelescope.com/astronomy-news/planck-upholds-standard-cosmology-0210201523/`, Feb 2015. Sky & Telescope.

[21] R. Sanders. Modified newtonian dynamics: A falsification of cold dark matter. *Advances in Astronomy*, 2009.

[22] Weinberg S. Bahcall J., Piran T. *Dark Matter In The Universe (Second Edition) 4Th Jerusalem Winter School For Theoretical Physics Lectures*. Wspc, 2004. ISBN 9812388419.

[23] Mamon G. Łokas E. Properties of spherical galaxies and clusters with an nfw density profile. *Monthly Notices of the Royal Astronomical Society*, 321(1):155–166, 2001.

[24] White S. Navarro J., Frenk C. The structure of cold dark matter halos. 1995.

[25] Flynn CH. Module 4: Mass models of galaxies. `http://www.astro.utu.fi/~cflynn/galdyn/lecture4.html`, March 2010. Lecture 1 : From the Big Bang to Stars.

[26] Gottlöber S. Ascasibar Y., Yepes G. On the physical origin of dark matter density profiles. *Monthly Notices of the Royal Astronomical Society*, 352(4):1109–1120, 2004.

[27] McMillan S. Computational physics: Leapfrog integrator. https://www.physics.drexel.edu/students/courses/Comp_Phys/Integrators/leapfrog/, 2017.

[28] Makino J. Hut P. The art of computational science. *The Kali Code. Internet source*, 2003.

[29] Glos V. *NFW hustotní profil temné hmoty a slupkové galaxie*. Bachelor's thesis, Masarykova univerzita, Přírodovědecká fakulta, Brno, 2015.